Pergamon

Phys. Chem. Earth (C), Vol. 24, No. 4, pp. 311–319, 1999

1464-1917/99/$ - see front matter

PII: S1464-1917(99)00004-5

Comparison between IRI and GPS-IGS Derived Electron Content during 1991–97

D. Bilitza[1], M. Hernández-Pajares[2], J. M. Juan[2] and J. Sanz[2]

[1]RSTX, Goddard Space Flight Center, Code 632, Greenbelt, MD 20771, U.S.A.
[2]Universitat Politècnica de Catalunya, Jordi Girona 1–3, Mod. C-3 / B-4, Campus Nord, 08034-Barcelona, Spain

Received 24 April 1998; accepted 21 August 1998

Abstract. The existence of a permanent network of GPS ground receivers, the *International GPS Service* (IGS), with available data since 1991, allows to perform an exhaustive comparison of the global electron content derived from these data using tomographic models with the International Reference Ionosphere (IRI) predictions. This work will allow the IRI upgrading for the electron content forecast, using this data set at global scale and along more than half solar cycle.

In this contribution we present a comparison involving more than 1300 stations *times* day worldwide distributed between 1991 (≃10 stations) and 1997 (≃200 stations).

1 Introduction

In the last years, the new possibility to estimate the global distribution of ionospheric -free- electrons by means of the Global Positioning System (GPS) has opened a very active and promising field of research, which can lead to important consequences, like:

- To help in providing a new and more accurate way of navigation for avionics (Hansen et al. 1997),
- To provide new views of the ionospheric storms that can be useful to improve its knowledge (Hernández-Pajares et al. 1998)
- To help in upgrading, and also to be helped, by the models describing the ionospheric electron content (Komjathy, Langley and Bilitza, 1998).

This last point is the framework of this paper: we are going to present the comparison between GPS electron content estimates and the International Reference Ionosphere (IRI, Bilitza, 1990) predictions[1] for different geomagnetic latitudes, since 1991. The GPS data have been gathered by the permanent network of GPS ground receivers, the *International GPS Service* (IGS, Zumberge et al., 1994).

In order to get the electron content (EC) estimates from GPS data, we must take into account some circumstances:

- The non-uniformity distribution of the GPS receivers (Hernández-Pajares et al. 1997) that can be appreciated in figure 1. This lack of stations is specially important near the geomagnetic equator, where the ionospheric EC present high gradients (reaching several TECU[2] per degree).
- Another problem falls in the mismodeling arena: usually the EC estimation is done assuming than the electron content is concentrated in a (thin) spherical layer at a fixed mean height (usually between 300 to 400 km) and estimating simultaneously the instrumental biases (of the receiver and transmitter) from the observed interfrequency aligned delays (L1-L2).

  This assumption implies several mismodeling effects:

  - The effective height can change 50-100 km between the night and day hemisphere (for instance looking at the maximum density height). This can 'charge' as horizontal gradients, vertical variations in electron content.
  - The plasmaspheric electron content is not modeled, and it can be at least the 10-20% of the TEC. A part of its electron content can be incorrectly charged to the instrumental delay estimates (until 1 TECU) due to the correlations.

We studied this problem in Juan et al. (1997) by means of a coarse 3-D tomographic model (2 layers in height corresponding to ionosphere and plasmasphere)

Correspondence to: M. Hernández-Pajares

[1]The newest version of the IRI –in May 1998– is used

[2]1 TECU = 10^{16} electrons/m^2 = 1.05 m of L1-L2 delay

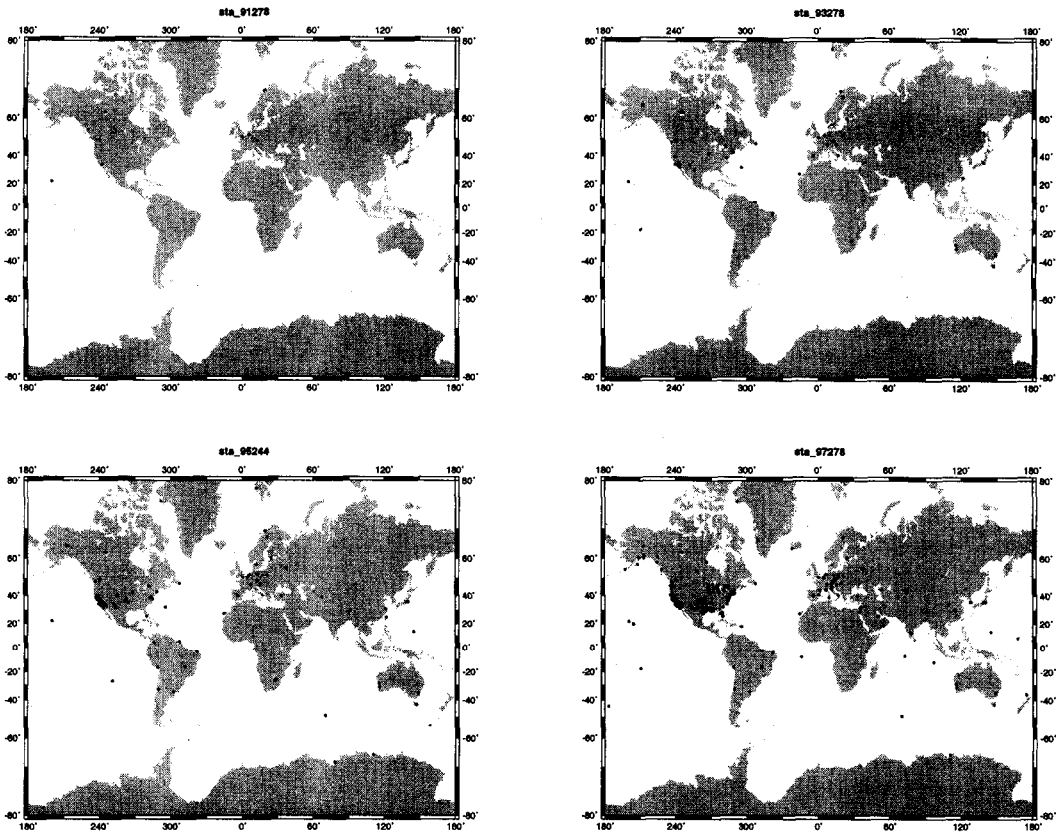

Fig. 1. Available IGS permanent GPS receivers in 4 epochs of the selected data set, separated by two years approximately. In particular they corresponds to October 5, 1991, October 5, 1993 (first row) and to September 1, 1995, October 5, 1997 (second row). These maps have been produced with the software package GMT, of Wessel & Smith, 1995.

solved during an ionospheric storm in November 15-19 1993, with the GPS IGS data in the North hemisphere.

As it was demonstrated using simulated data by Hajj et al. (1994) and recently by Howe et al. (1998), one way of improving the vertical resolution of the tomographic model, and hence to reduce the mismodeling of the EC estimates, is to use not only ground observations -with typical 'radial' geometry- but also observations taken in occultation scenarios from on-board GPS receivers in Low Earth Orbiter (LEO), such the GPS/MET. We presented a study in this direction with true data geometry (4 spherical layers), in Hernández-Pajares et al. (1996), and the computation of global tomographic GPS models with real data during ionospheric storms in Hernández-Pajares et al. (1998).

2 The model

2.1 The carrier phase preprocessing

The geodetic dual frequency GPS receivers usually provides, for each epoch and for each of the tracked satellites -typically 6 or 7 simultaneously-, *code phases* (P_1 and P_2)[3] and *carrier phases* ($\mathcal{L}_1$ and $\mathcal{L}_2$) in two L-band frequencies $f_1 \simeq 1575$ MHz and $f_2 \simeq 1227$ MHz respectively. The carrier phases are very accurate with errors of 0.002 m or smaller (Wells et al. 1986, page 9.14), being the result of the correlation between the incoming carrier with the receiver replica.

The GPS signals travel between the transmitter position $\vec{r}^T(t^T)$ and the receiver position $\vec{r}_R(t_R)$, crossing regions of the ionosphere with densities N_e. Then the main ionospheric quantity obtained from the dual frequency GPS receiver data is the ionospheric combination of carrier phases, $\mathcal{L}_I \equiv \mathcal{L}_1 - \mathcal{L}_2$, that can be written in terms of:

$$\mathcal{L}_I = \kappa \cdot \int_{\vec{r}^T(t^T)}^{\vec{r}_R(t_R)} N_e(\vec{r},t)\, ds + D_R + D^T + \lambda_1 \cdot N_1 - \lambda_2 \cdot N_2 + \epsilon_I$$

where $D_R = D_{1,R} - D_{2,R}$ and $D^T = D_1^T - D_2^T$ are the inter-frequency biases for receiver R and transmitter T, $\kappa = K\left[1/f_2^2 - 1/f_1^2\right] \simeq 1.0506$ m delay/10^{17} electrons/m^2 and $\sigma_{\epsilon_I} \simeq \sigma_{\epsilon_1} \simeq \sigma_{\epsilon_2} \simeq 0.002m$.

Finally, it remains yet the integer ambiguities term $\lambda_1 \cdot N_1 - \lambda_2 \cdot N_2$, that is constant within each arc of connected carrier phases (without "cycle-slips", see Blewitt, 1990). To cancel it [4] we consider differences between continuous phases for the same pair of transmitter T and receiver R differing in τ seconds. This time must be sufficient to provide enough geometry variation of the ray to allow solving for the free electron densities in the tomographic problem and small enough to suppose that the electron density does not change in a reference frame with the Sun fixed (for instance, for $\tau \geq 720$ seconds the method works well).

Then, the final equation in the preprocessing stage is:

$$\mathcal{L}_I(t+\tau) - \mathcal{L}_I(t) = \\ = \kappa \cdot \left(\int_{\vec{r}^T(t^T+\tau)}^{\vec{r}_R(t_R+\tau)} N_e(\vec{r},t)\, ds - \int_{\vec{r}^T(t^T)}^{\vec{r}_R(t_R)} N_e(\vec{r},t)\, ds \right) + \epsilon_I \quad (1)$$

2.2 The tomographic equation

We decompose the ionosphere in 3-D cells in the Sun fixed reference frame "local time/geodetic latitude/height" (see below). In these cells we assume that the electron density is constant (see figure 2). Then the last equation (1) becomes, for each arc of continuous carrier phases between a transmitter T and receiver R:

$$\mathcal{L}_I(t+\tau) - \mathcal{L}_I(t) = \\ = \kappa \sum_i \sum_j \sum_k (N_e)_{i,j,k} \cdot \left[\Delta s_{i,j,k}^{t+\tau} - \Delta s_{i,j,k}^{t} \right] + \epsilon_I \quad (2)$$

where i, j, k are the indices for each cell corresponding to local time, geodetic latitude and height; $(N_e)_{i,j,k}$ is the corresponding free electron density; and $\Delta s_{i,j,k}^t$ is the length of the ray path crossing the illuminated cells at time t ($\Delta s_{i,j,k}^t = 0$ for the "dark" cells).

3 Computations and Results

The number of IGS stations have increased dramatically since 1991 until now (see figure 1). So in order to extent our comparison between GPS estimates and IRI predictions, to the beginning of nineties –close to the last solar maximum– with few available stations, we are going to solve our tomographic model station by station.

We consider a tomographic model like in figure 2 but only with 2 layers due to the limitations of the ray geometry (from one single station). The GPS model consists on 48×5×2 cells in local time, latitude and height, where we assume that the electron density is constant. They are solved independently for each receiver during one day of data. The resolution in local time is 7.5 degrees (half hour), 5 degrees in latitude. The two layers are delimited by three spherical shells at 60, 740 and 1420 km.

Only the results of the (central) latitude band above each station will be considered.

3.1 Model assessment

To assess the capability to solve the model, we have generated semisynthetic data sets, that can be used as "calibration functions" of the model:

- The rays are those corresponding to the IGS stations FORT (Fortaleza, Brazil at geomagnetic coordinates (32,-5) degrees) and MADR (Madrid, Spain at

[3] With P codes encryption, or Anti-Spoofing, the C/A code and a pseudo-P_2 are used instead of P_1 and P_2.

[4] Notice that in this way we avoid to align with the code to estimate this ambiguity term, and then we avoid the associated alignement error, specially important now with the Anti-Spoofing activated ($\simeq$ 0.3m).

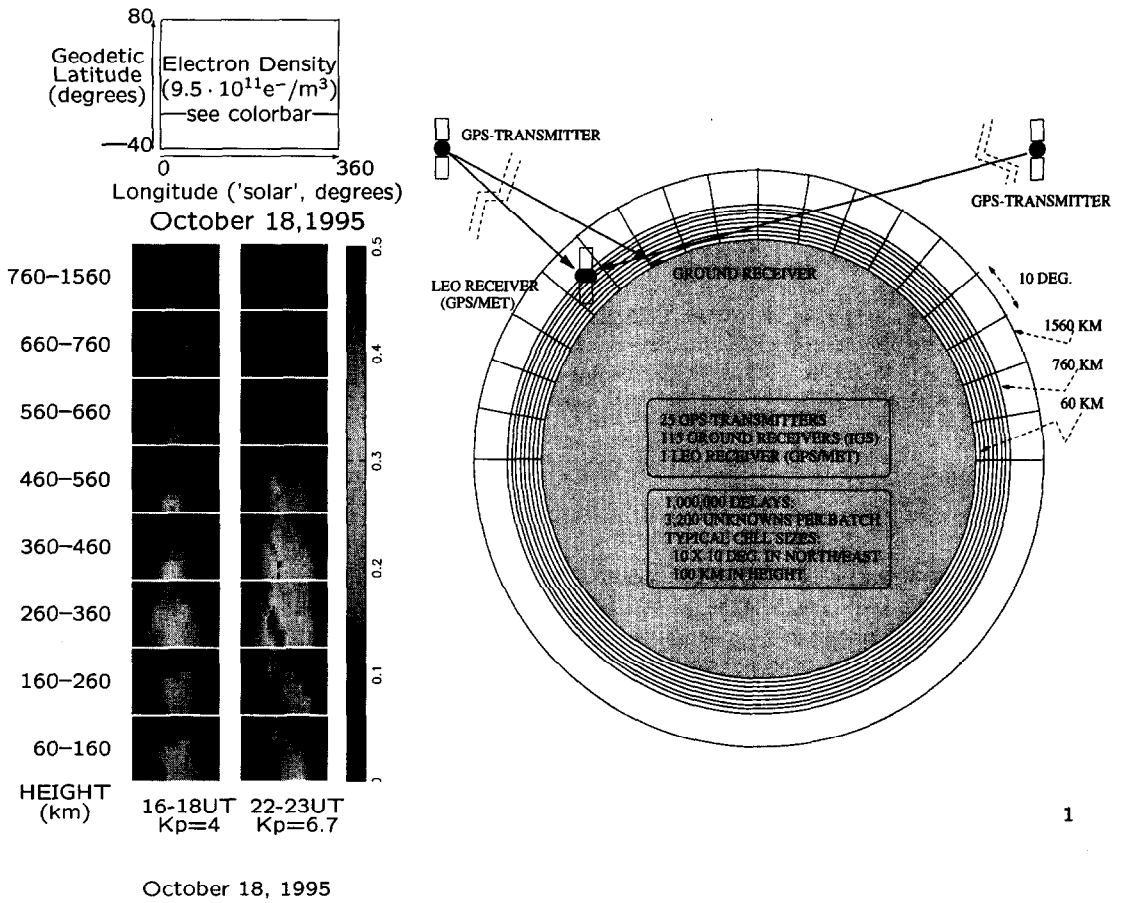

Fig. 2. Layout of a typical tomographic model (8 layers) solved with ground and LEO GPS data (right) –see details in Hernández-Pajares et al. 1998–. One sample of these results are indicated in the left, plotting the mean electronic density estimation during two epochs of the geomagnetic storm of October 18-19, 1995 (left, first and second column of plots). Each row correspond to each one of the eight layers from bottom to top. Each image represents the global electron density estimate corresponding to the given epoch (column) and layer (row) for all the local times (X-axis) and for latitudes between -40 and 80 degrees (Y-axis).

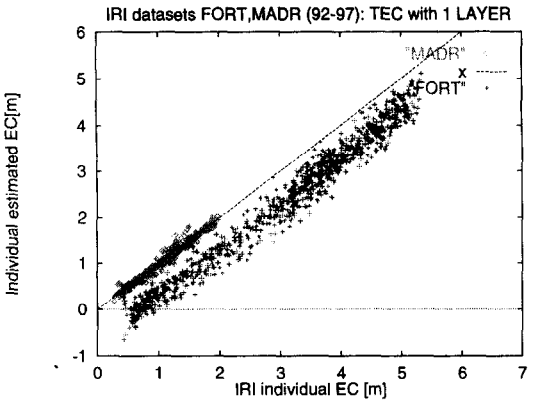

Fig. 4. Calibration of the one-layer GPS model with boundaries at heights of 60 and 740 km. It is evident the mismodelling in the equatorial station FORT (≃0.5 meters) several times greater than the mismodelling in the two-layer model (second plot of figure 3).

geomagnetic coordinates (75,44) degrees) when they have been available in the dataset (table 1).

- The observed ionospheric delays have been substituted by the IRI predicted delays for each observation.

To summarize the agreement between the estimation and the reference IRI EC we show in figure 3 (first column) one point per station and day, representing the mean of the estimated EC in function on the reference ("true") mean IRI EC (Total TEC, first layer PTEC1 and second layer PTEC2).

The error bar represents the standard deviation (RMS) of the difference between the estimated and the "true" EC, cell by cell.

We can see that the mean TEC is well recovered with discrepancies of few TECU and with RMS also below few TECU[5]. The values estimated for the bottomside EC tend to be a bit smaller than the "true" (IRI) ones for large EC values. The reciprocal effect is more clear in the topside EC, with recovered values until 5 TECU greater than the reference ones. This is due to the correlation between the topside and bottomside estimation using only ground data.

The corresponding plots for the individual electron content estimates and its formal errors, instead of the daily means and RMS, are in the second column of figure 3 where these results can be better observed. It is shown a better retrieval than the "classical" one layer model (figure 4).

3.2 Real data

We have preprocessed the observations corresponding to all the available IGS stations for 23 days since 1991 to 1997.

The general criterium has been to select one day for each month of January, March, July and October[6], the most geomagnetically quiet day of the first 5. The selected days jointly with the mean Ap index and the number of stations analyzed (and preprocessed) are indicated in table 1.

Finally, for these data sets, only the stations with continuous GPS observations during the entire day have been analyzed.

In figure 5 the mean GPS estimations and RMS of the difference GPS-IRI are plotted in function on the mean IRI predicted values (diamonds) for the real data (one point represents the estimation of one station during one day). The crosses represent the "GPS calibration function" discussed previously. We can see that the mean GPS and IRI TEC agree well for mean IRI values below 2 m (at the level of 0.2 m -2 TECU-), i.e. for the 95% of the stations × day processed. Between 2 and 4 m (4% of points) the GPS mean TEC estimates are in general below the IRI prediction (with some higher values), and for values greater than 4 m (1% of station × day) we enter in the non GPS calibrated range, corresponding

Table 1. List of days of the IGS selected data indicating also the mean Ap, and the number of the analyzed stations and the number of preprocessed ones (with dual frequency code receivers).

Year	DOY	Month	Day	Ap mean	Nbr.sta.
1991	186	July	5	4	2(7)
1991	278	October	5	15	5(10)
1992	001	January	1	12	10(16)
1992	065	March	5	12	11(16)
1992	186	July	4	4	12(26)
1992	279	October	5	5	12(27)
1993	001	January	1	10	17(29)
1993	064	March	5	7	22(33)
1993	186	July	5	5	28(40)
1993	278	October	5	5	43(49)
1994	005	January	5	4	44(50)
1994	063	March	4	4	36(46)
1994	186	July	5	5	56(64)
1994	274	October	1	4	40(46)
1995	001	January	1	4	65(77)
1995	062	March	3	6	64(83)
1995	186	July	5	3	96(112)
1995	244	September	1	4	91(115)
1996	004	January	4	5	100(116)
1996	062	March	2	3	135(158)
1996	184	July	2	6	135(161)
1997	004	January	4	4	159(184)
1997	278	October	5	2	199(240)

[5] Some large RMS are due to few bad electron content estimations that are not used to weight the means in this comparison.

[6] The exception has been September of 1995, because there were not broadcast ephemeris available for October 1995, and January 5 1991, October 5 1996, March 4 1997 and July 1 1997 that have not been processed due to other problems.

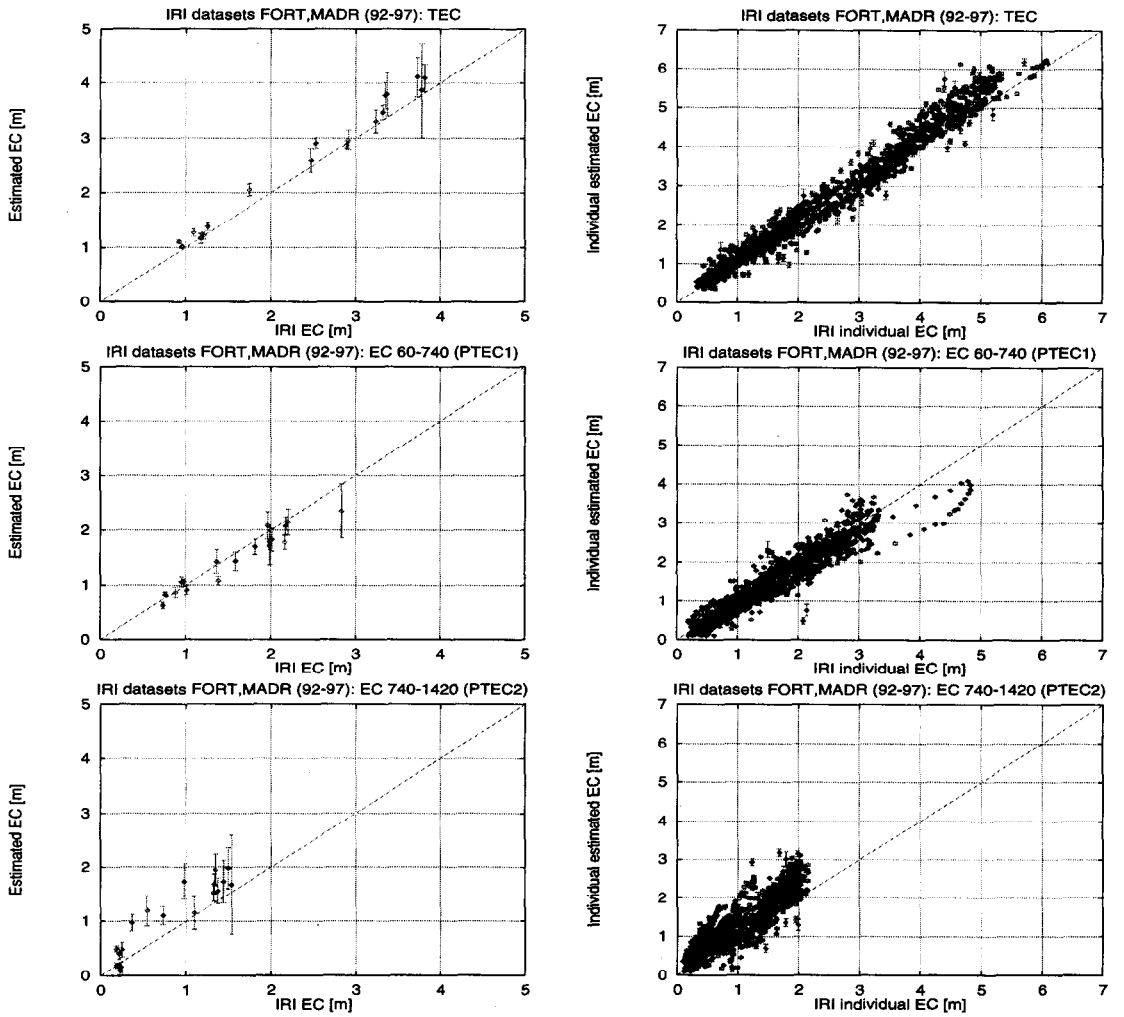

Fig. 3. Calibration of the GPS tomographic model solved station by station: (1) In the first column, the X-axis represents the mean IRI Electron Content (the reference values) for each station, processed independently each day, being the IRI the reference model used to generate the semisynthetic data set. The Y-axis runs the 'station-daily' mean of the estimated values with GPS. (2) In the second column the values X and Y refer to the individual IRI values and estimates for each estimated cell. The geometry is the true one. The error bar represents the RMS of the differences between the estimated and the reference values for each station in the first column and the formal error in the second column. The three rows correspond to the TEC, bottomside EC and topside EC respectively. The dotted line represents the ideal case: to retrieve exactly the IRI, the reference in this calibration study.

the points with higher mean IRI values to IGS stations *yell* and *trom* at 69 and 67 deg of geomagnetic latitude, respectively.

For the mean partial electron content for the first layer at 60-740 km (PTEC1) and the second layer (740-1420 km, PTEC2), we can see that there is a reasonable agreement for PTEC1. But for PTEC2, and for mean IRI values between 1 and 2 m, the GPS estimates are lower (near the half) than the IRI predicted values for the topside electron content.

Referring to the RMS also plotted in figure 5, it seems that there are in general some significant differences between IRI and GPS, reaching sometimes 3-4 times the intrinsic RMS of the GPS model ($\leq$ 0.5 meters).

To finish this section to say that in despite of that the more noticcable difference, afecting to 1% of the points, is the low mean TEC (and PTEC2) estimated by GPS for high mean IRI values (basically for the data of 1991 and beginning of 1992), it happens outside the range covered by the present calibration. The GPS mean TEC values (4%) that are lower than the IRI prediction for the top band of the calibrated GPS range in figure 5 (2-4 m) may be due to the limitations of the GPS tomographic model described in subsection 3.1, or it might be due to an overestimation of real EC by the IRI model. It must be taken into account the selection criteria with quiet geomagnetic days for this study, and the fact that the IRI provides (by default) the prediction depending on the mean Sun Spot Number, smoothed along one year of time.

4 Conclusions

We have presented the first results of an exhaustive comparison of the electron content estimated with GPS and the IRI prediction during 23 geomagnetically quiet days distributed between 1991 and 1997 for the the most part of the available IGS stations and the associated (full) range of geomagnetic latitudes. Starting from near 1 Gigabyte of compressed GPS raw data, we have analyzed the results of 1382 stations $\times$ day, with 3,000,000 of observations.

The tomographic GPS model has been solved independently station by station for each daily dataset. This has allowed to extent the comparison to the oldest available IGS data, where few GPS receivers were working continously.

The GPS model has been "calibrated" by mean of some representative semysinthetic data subsets.

The mean GPS estimate of the TEC (and bottomside electron content) are in general quite compatible with the IRI prediction (95% of the processed stations $\times$ day) at the level of 2 TECU. The lower mean values obtained with GPS, in the top band of the GPS calibrated range, need further investigation.

Regard to the GPS estimates and the IRI electron content distributions, our RMS study indicates that they present some meaningful differences.

The GPS model exposed in this paper is presently used by the UPC authors to generate (in ionex format) the global TEC estimation from IGS GPS data at planetary scale, with a final resolution of 2 hours $\times$ 5 degrees $\times$ 2.5 degrees in UT $\times$ longitude $\times$ latitude (see Web document http://maite152.upc.es /~ionex/gAGE_dip/gAGE_dip.html). This is done every day, since June 1st 1998, being the UPC one of the IGS Ionosphere Associated Analysis Centers involved in the effort to create a common IGS ionospheric product (see the position paper Feltens & Schaer, 1998).

Acknowledgements. We acknowledge to the IGS for the availability of the data, and in particular to the University of California, San Diego, that have put online the most part of the IGS data since 1991 until now. This work has been partially supported by the Spanish CICYT project TIC97-0993-C02-01 and by the fellowships PR97-38426973 and PR97-37733675 and NSF grant ATM-9713469.

References

Bilitza D., International Reference Ionosphere 1990. URSI/COSPAR, NSSDC/WDC-A-R&S 90-22, 1990.

Blewitt G., An automatic editing algorithm for GPS data, *Geophys. Res. Lett., 17*, 199-202, 1990.

Feltens, J. and S. Schaer, IGS products for the ionosphere, Proceedings of the IGS Analysis Center Workshop, ESA/ESOC Darmstadt, Germany, 225-232.

Hajj, G.A., R. Iba nez-Meier, E.R. Kursinski and L.J. Romans, Imaging the ionosphere with the Global Positioning System, Imaging Syst. Technol., 5, 174-184, 1994.

Hansen A.J., T. Walker and P. Enge, Ionospheric Correction Using Tomography, Proceedings of the Institute of Navigation GPS'97, September 97, Kansas City, USA, 1997.

Hernandez-Pajares M., J.M. Juan and J. Sanz, Application of Kohonen maps to the GPS Stochastic Tomography of the Ionosphere, "Data Science, Classification, and Related Methods" ISBN 4-431-70208-3 Springer-Verlag Tokyo, p. 341-350. , Fifth Conference of the International Federation of Classification Societies (IFCS-96), Kobe, Japan, March 27-30, 1996.

Hernandez-Pajares M., J.M. Juan and J. Sanz, Neural network modeling of the ionospheric electron content at global scale using GPS data, Radio Sci., 32, 1081-1090, 1997a (also available at http://maite152.upc.es/ manuel/tecada10/tecada10.html).

Hernandez-Pajares M., J.M. Juan, J. Sanz and J.G. Solé, Global observation of the ionospheric electronic response to solar events using ground and LEO GPS data, Journal of Geophysical Research – Space Physics, 103, 20789-20796, 1998.

Howe B. M., K. Runciman and J. A. Secan, Tomography of the ionosphere: Four-dimensional simulations, Radio Sci., 33 , 109-128, 1998.

Juan J.M., A. Rius, M. Hernandez-Pajares, J. Sanz, A two-layer model of the ionosphere using Global Positioning System data. Geophys. Res. Lett., 24, 393-396, 1997

Komjathy A., R.B. Langley and D. Bilitza, Ingesting GPS-Derived TEC Data into the International Reference Ionosphere for Single Frequency Radar Altimeter Ionospheric Delay Corrections, Adv. Space Res., 22, N.6, 793-801, 1998.

Wells D. et al., Guide to GPS Positioning, Canadian GPS Associates, Fredericton N.B., Canada, 1986.

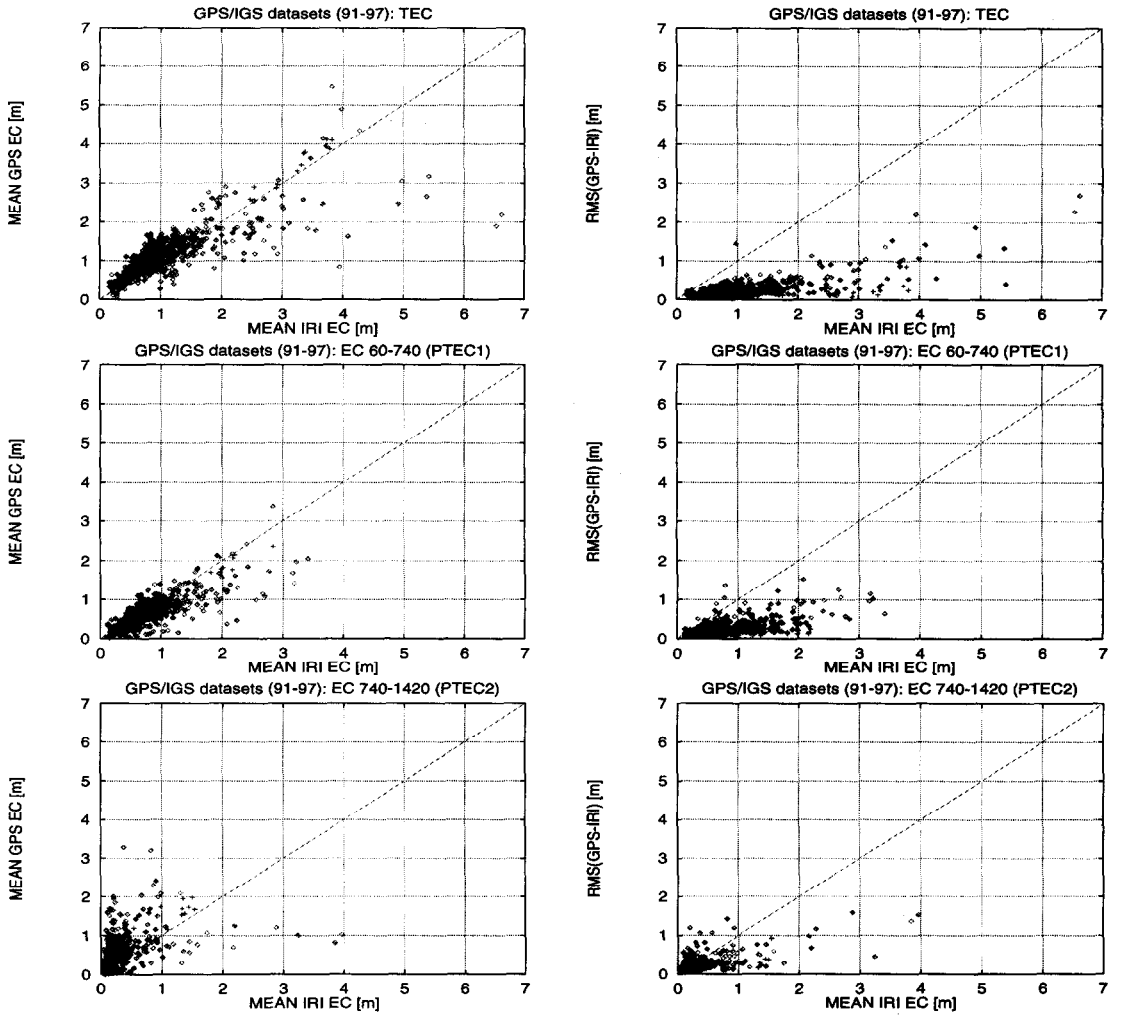

Fig. 5. The first column of plots represents the mean of the estimated EC with GPS with the real data vs. the mean of the IRI prediction (TEC, bottomside and topside electron content respectively). The second column of plots represents the corresponding RMS of the differences GPS-IRI. The values obtained in the GPS model calibration are superimposed. The dotted line represents when GPS estimates would be equal to IRI prediction in the case of the mean TEC (first column) and it represents when the RMS equals to the mean IRI TEC value for the RMS plots (second column).

Wessel P. and W.H.F. Smith, New version of the Generic Mapping Tools released, *EOS Trans. AGU*, 76, 326, 1995.
Zumberge, J., R. Neilan, G. Beutler, and W. Gurtner, The International GPS Service for Geodynamics-Benefits to Users, paper presented at the Institute of Navigation GPS-94 Meeting, Salt Lake City, Utah, Sept. 20-23, 1994.